THE ASTROPHYSICAL JOURNAL, 425:222–230, 1994 April 10

STANDARD AND NONSTANDARD PLASMA NEUTRINO EMISSION REVISITED

MARTIN HAFT AND GEORG RAFFELT
Max-Planck-Institut für Physik, Föhringer Ring 6, 80805 München, Germany
AND
ACHIM WEISS
Max-Planck-Institut für Astrophysik, 85748 Garching, Germany
Received 1993 July 12; accepted 1993 September 16

ABSTRACT

On the basis of Braaten & Segel's representation of the electromagnetic dispersion relations in a QED plasma, we check the numerical accuracy of several published analytic approximations to the plasma neutrino emission rates. As we find none of them satisfactory, we derive a new analytic approximation which is accurate to within 4% where the plasma process dominates. The correct emission rates in the parameter regime relevant for the red giant branch in globular clusters are larger by about 10%–20% than those of previous stellar evolution calculations. Therefore, the core mass of red giants at the He flash is larger by about 0.005 $M_\odot$, or 1%, than previously thought. Our bounds on neutrino magnetic dipole moments remain virtually unchanged.

Subject headings: elementary particles — plasmas — radiation mechanisms: nonthermal — stars: giants — stars: interiors

1. INTRODUCTION

In stars with densities below nuclear, neutrinos are emitted by the plasma process $\gamma \to \bar{\nu}\nu$, the photo process $\gamma e^- \to e^- \bar{\nu}\nu$, the pair process $e^- e^+ \to \bar{\nu}\nu$, and by bremsstrahlung $e^-(Ze) \to (Ze)e^- \bar{\nu}\nu$. In Figure 1 we show the regions of density and temperature where each of these processes dominates over the others. The plasma process is particularly interesting because it does not occur in vacuum and yet dominates the stellar emission rates in a large range of temperatures and densities. Notably, white dwarfs and the degenerate cores of low-mass red giants fall in this parameter region. Evolutionary calculations for these stars can be tested with great statistical significance. For example, globular cluster observations allow one to determine the core mass at the helium flash to within about 0.012 $M_\odot$, or 2.5% at a 1 σ statistical confidence level (Raffelt 1990; Raffelt & Weiss 1992). Therefore, it is important to identify possible systematic effects that would enter at this or at a larger level. If the standard neutrino loss rates are multiplied by a factor F_ν, where $F_\nu = 1$ refers to the standard case, the core mass at the helium flash varies approximately as $\delta M_c = 0.020\ M_\odot\ \delta F_\nu$. This strong sensitivity to the neutrino luminosity has been used to constrain possible nonstandard contributions such as the plasmon decay by virtue of neutrino dipole moments (Raffelt 1990; Raffelt & Weiss 1992).

In practical stellar evolution calculations the neutrino loss rates are implemented in the form of simple analytic approximations. Widely used versions are those of Beaudet, Petrosian, & Salpeter (1967), Munakata, Kohyama, & Itoh (1985), Schinder et al. (1987), and Itoh et al. (1989). With regard to the plasma process, the results of Beaudet et al., Munakata et al., and Schinder et al. agree with one another to better than 1% if the same neutrino coupling strength to electrons is used, while Itoh et al. made an attempt to improve the accuracy of the rates at low temperatures.

It turns out that all of these rates are relatively poor approximations for $T \lesssim 10^8$ K, which is relevant for low-mass stars. They were optimized for higher temperatures and correspondingly higher densities in the diagonal band of Figure 1 where the plasma process dominates. At higher densities, however, the approximate photon dispersion relation that had been used in all of these works is a rather poor approximation (Braaten 1991), with the result that the above plasma emission rates are bad approximations everywhere. In response, Itoh et al. (1992) have derived a new analytic formula which is claimed to fit the exact results to better than 5% in the region where the plasma process dominates. Independently, Blinnikov & Dunina-Barkovskaya (1992) have published rates which were optimized for low-mass stars.

Since then, Braaten & Segel (1993) have devised an approach to the photon dispersion relation which, for given T and ρ, reduces the calculation of the plasma emission rate essentially to the numerical evaluation of a few one-dimensional integrals. Their method offers for the first time a simple and practical approach to check the accuracy of all of the above emission rates as well as the approximations that were used to study nonstandard neutrino emission (Raffelt 1990; Raffelt & Weiss 1992; Blinnikov & Dunina-Barkovskaya 1992; Castellani & Degl'Innocenti 1992). On the basis of this method we found none of the above approximations satisfactory and thus have derived a new analytic approximation to the standard rate for the plasma process which is accurate to better than 4%. For the nonstandard emission rates we found that a simple scaling of the standard rates as in Raffelt & Weiss (1992) introduces only a small error (less than 5%) for low-mass stars, so that bounds on neutrino dipole moments are mostly affected by the accuracy of the standard emission rates.

We begin in § 2 by adapting the results of Braaten & Segel (1993) to our calculation of standard and nonstandard emission rates by the plasma process. Besides the standard neutrino interactions we include the possibility of the coupling of right-handed neutrinos to electrons (Fukugita & Yanagida 1990), neutrino dipole moments, and neutrino electric "millicharges." In § 3 we perform a numerical test of all of the above analytic approximations, and we derive and test a new version. We also

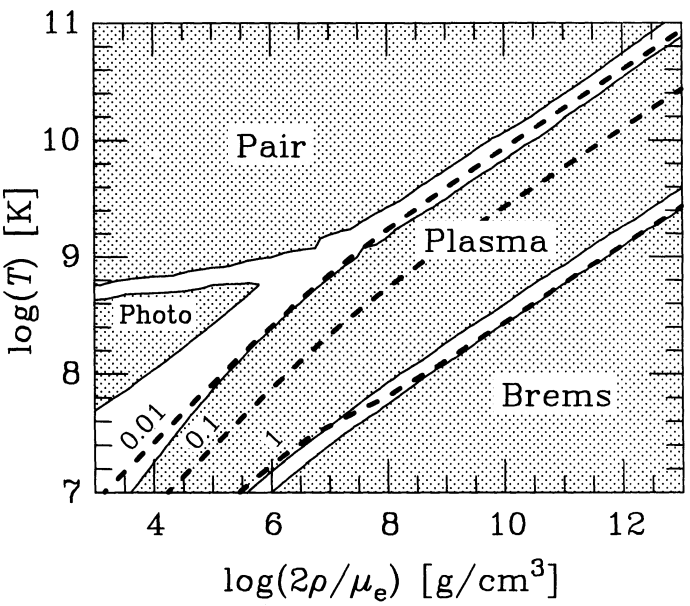

FIG. 1.—Regions of density and temperature where the different neutrino emission processes contribute more than 90% of the total; μ_e is the mean number of baryons per electron. The bremsstrahlung contribution is for helium. The dashed lines are contours for the indicated values of Q_L/Q_T, i.e., the contribution of the longitudinal relative to the transverse plasma process.

check the accuracy of a simple scaling of the standard rates to obtain the nonstandard ones. In § 4 we discuss the accuracy of previous calculations of the core mass at the helium flash as well as the accuracy of previous bounds on neutrino properties, and we derive bounds on the Fukugita & Yanagida model as well as on neutrino millicharges.

2. EXACT EMISSION RATES

2.1. *Electromagnetic Excitations in a Medium*

The behavior of electromagnetic excitations in a linear medium is best understood on the basis of the wave equation for the vector potential A in Feynman gauge, $(K^2 - \Pi)\, A = j_{\rm ext}$, where $j_{\rm ext}$ is an external electromagnetic current and Π is the polarization tensor. Moreover, $K^2 = \omega^2 - k^2$, where ω is the frequency while $k = |\boldsymbol{k}|$, the modulus of the momentum coordinate. In an isotropic medium which also remains invariant under a parity transformation, the polarization tensor can be expressed as (Nieves & Pal 1989a, b) $\Pi = \pi_T Q_T + \pi_L Q_L$, where Q_T is a K-dependent projector on the subspace transverse to $\boldsymbol{k}$, while Q_L projects on the longitudinal subspace, and in addition $Q_{T,L} K = 0$, so that $\Pi K = 0$ as required by gauge invariance. Explicit expressions for $Q_{T,L}$ in terms of K were given, for example, by Weldon (1982). He also showed that in the rest frame of the medium $\pi_L = -\Pi_{00} K^2/k^2$ and $\pi_T = (\Pi^\mu_\mu - \pi_L)/2$.

If Π is expressed in this way, it is clear that the homogeneous wave equation $(K^2 - \Pi)A = 0$ has nontrivial solutions only for

$$\omega^2 - k^2 - \pi_s(\omega, k) = 0\,, \quad s = T \text{ or } L\,, \tag{1}$$

a relationship which implicity defines the dispersion relations for transverse and longitudinal propagating modes ("photons" and "plasmons" or "transverse and longitudinal plasmons").

In order to calculate the decay rate into neutrinos of such modes, we need to normalize properly the amplitude of the quantized excitations. To this end, we consider a mode k, polarization $s = T$ or L, with the corresponding frequency $\omega_{s,k}$ so that the dispersion relation in equation (1) is obeyed. Then we expand $\pi_s(\omega, k) = \pi_s(\omega_{s,k}, k) + \partial_{\omega^2}\pi_s(\omega_{s,k}, k)(\omega^2 - \omega^2_{s,k})$ so that the equation of motion for the amplitude $A_{s,k}$ is that of a harmonic oscillator. Equivalently, we write the photon propagator near its poles in the form $Z_s/(\omega^2 - \omega^2_{s,k})$. Either way, one finds that the squared matrix element of a process with an external electromagnetic excitation of momentum k and polarization s carries a factor

$$Z_s = [1 - \partial_{\omega^2}\pi_s(\omega_{s,k}, k)]^{-1}\,. \tag{2}$$

In a fully ionized plasma the polarization tensor is simply given in terms of the forward-scattering amplitudes of photons on the electrons and positrons. To lowest order in $\alpha = e^2/4\pi$, it is found to be

$$\Pi_{\mu\nu} = -8\pi\alpha \int \frac{d^3\boldsymbol{p}}{(2\pi)^3}\frac{f(E_p)}{E_p} \times \frac{P\cdot K(K_\mu P_\nu + K_\nu P_\mu) - K^2 P_\mu P_\nu - (P\cdot K)^2 g_{\mu\nu}}{(P\cdot K)^2 - K^4/4}\,, \tag{3}$$

where $P = (E_p, \boldsymbol{p})$ is an e^- or e^+ four-momentum. The sum of the phase-space occupation numbers for these particles is

$$f(E) = \frac{1}{e^{(E-\mu)/T} + 1} + \frac{1}{e^{(E+\mu)/T} + 1}\,, \tag{4}$$

with μ the electron chemical potential and T the temperature. On the basis of equation (3) it is, in principle, straightforward to derive π_s and Z_s for a given μ and T.

2.2. *Analytic Representation for* Π *and* Z

Braaten & Segel (1993) have shown that ignoring the $K^4/4$ term in the denominator of equation (3) introduces an error which appears only on the α^2 level, so that to $O(\alpha)$ it can be ignored. In fact, ignoring this term provides a *better* approximation to the $O(\alpha)$ result than keeping it, because π_T then remains real for all conditions, as it must because the imaginary part from the $\gamma_T \to e^+e^-$ process which otherwise appears at sufficiently large plasma frequencies is unphysical (Braaten 1991).

Once the $K^4/4$ term has been dropped, the angular part of the integral in equation (3) can be done analytically, leaving one with a one-dimensional integral over electron momenta which can be done analytically in the classical, degenerate, and relativistic limit. In these cases Braaten & Segel found[1]

$$\begin{aligned}\pi_T(\omega, k) &= \omega_P^2[1 + \tfrac{1}{2}G(v_*^2 k^2/\omega^2)]\,,\\ \pi_L(\omega, k) &= \omega_P^2[1 - G(v_*^2 k^2/\omega^2)] + v_*^2 k^2 - k^2\,,\end{aligned} \tag{5}$$

where $v_* \equiv \omega_1/\omega_P$ has the interpretation of a typical velocity of the electrons in the medium. The plasma frequency ω_P and the

[1] Braaten & Segel used Coulomb rather than Feynman gauge, so that we had to translate their longitudinal expression accordingly. We preferred to follow Weldon (1982) in the choice of gauge because the dispersion relations and plasmon decay rates then have the same form for transverse and longitudinal excitations.

frequency ω_1 are defined by

$$\omega_P^2 \equiv \frac{4\alpha}{\pi}\int_0^\infty dp\left(v-\frac{1}{3}v^3\right)pf(E_p)\,,$$
$$\omega_1^2 \equiv \frac{4\alpha}{\pi}\int_0^\infty dp\left(\frac{5}{3}v^3-v^5\right)pf(E_p)\,, \tag{6}$$

where $v = p/E_p$ is the electron or positron velocity. In the classical limit one has $v_* = (5T/m_e)^{1/2}$, in the degenerate limit $v_* = v_F$ (velocity at the Fermi surface), and in the relativistic limit $v_* = 1$. The function G is defined by

$$G(x) \equiv \frac{3}{x}\left[1-\frac{2x}{3}-\frac{1-x}{2x^{1/2}}\log\left(\frac{1+x^{1/2}}{1-x^{1/2}}\right)\right]$$
$$= 6\sum_{n=1}^{\infty}\frac{x^n}{(2n+1)(2n+3)}\,. \tag{7}$$

We have plotted $G(x)$ in Figure 2; note that $G(0) = 0$, $G(1) = 1$, and $G'(1) = \infty$.

Braaten & Segel then claim (and we have checked) that these results apply approximately for all conditions. The deviations between $\pi_s(\omega, k)$ given by equation (5) and by the proper integral over the e^+e^- phase space are always so small that equation (5) can be considered exact to $O(\alpha)$. Because a higher precision would require an $O(\alpha^2)$ QED calculation, nothing is gained by evaluating the full integrals. Therefore, the above results are as exact as an $O(\alpha)$ result can be.

In order to calculate the plasmon decay rates, we also need the amplitude normalization factors. Braaten & Segel (1993) found the analytic representations

$$Z_{T,k} = \frac{2\omega_{T,k}^2(\omega_{T,k}^2 - v_*^2k^2)}{\omega_{T,k}^2(3\omega_P^2 - 2\pi_{T,k}) + (\omega_{T,k}^2 + k^2)(\omega_{T,k}^2 - v_*^2k^2)}\,,$$
$$Z_{L,k} = \frac{2\omega_{L,k}^2(\omega_{L,k}^2 - v_*^2k^2)}{[3\omega_P^2 - (\omega_{L,k}^2 - v_*^2k^2)]\pi_{L,k}}\,. \tag{8}$$

In these expressions $\pi_{s,k} \equiv \pi_s(\omega_{s,k}, k)$ is the "on-shell" value of π_s for excitations with momentum k, i.e., $\omega_{s,k}^2 - k^2 = \pi_{s,k}$.

The decay $\gamma_s \to \bar{\nu}\nu$ is only possible if γ_s has a timelike four-momentum, $\omega_{s,k} > k$. For longitudinal excitations this condition is only fulfilled for $k < k_{\max}$, where

$$k_{\max} = \omega_P\left\{\frac{3}{v_*^2}\left[\frac{1}{2v_*}\log\left(\frac{1+v_*}{1-v_*}\right)-1\right]\right\}^{1/2} \tag{9}$$

to the same level of approximation.

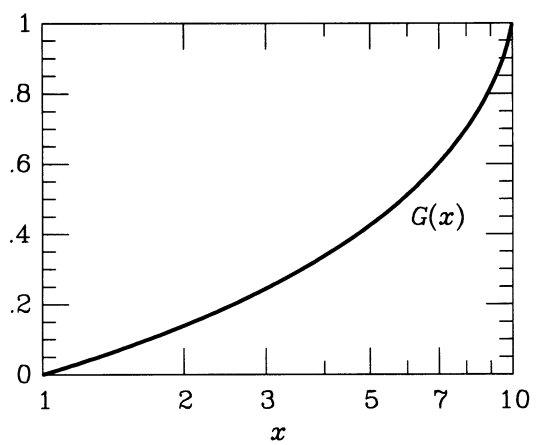

FIG. 2.—Function $G(x)$ as defined in eq. (7)

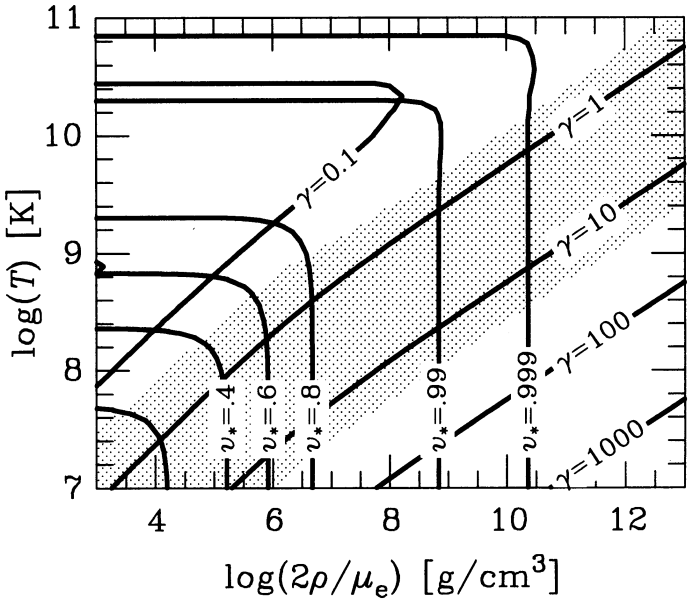

FIG. 3.—Contours of $\gamma = \omega_P/T$ and v_* as defined in eq. (6)

In the Braaten & Segel representation the on-shell values $\pi_{s,k}$ and thus the dispersion relations depend only on the medium parameters ω_P and v_*. However, media are more readily characterized by their density and temperature. Therefore, in Figure 3 we show contours of constant v_* and $\gamma \equiv \omega_P/T$ in the region of ρ and T relevant for the plasma process in stars. In the shaded area the plasma process contributes more than 10% to the total neutrino luminosity. Evidently, it is important only for $0.3 \lesssim \gamma \lesssim 30$. Moreover, the v_* contours are almost perfect vertical straight lines in this regime, i.e., the medium is degenerate.

The polarization functions $\pi_{s,k}/\omega_P^2$ and the amplitude factors $Z_{s,k}$ are functions only of v_* and of k/ω_P. In Figure 4 we show contours for these functions in the (v_*, k)-plane for transverse excitations. We have $1 < \pi_{T,k}/\omega_P^2 < 3/2$ and $Z_{T,k} < 1$. The deviation of $Z_{T,k}$ from unity is always small. In Figure 5 we show similar contours for the longitudinal case. We have $\pi_{L,k}/\omega_P^2 < 1$; the occurrence of the plasma process in addition requires $0 < \pi_{L,k}$. The contour $\pi_{L,k} = 0$ is identical with the function $k_{\max}(v_*)$ given in equation (9). The amplitude function $Z_{L,k}$ diverges when $k \to k_{\max}$. Therefore, we show in Figure 5 (*lower panel*) contours for $Z_{L,k}^* \equiv Z_{L,k}\,\pi_{L,k}/\omega_{L,k}^2$ instead.[2]

2.3. *Plasmon Decay Rates*

In order to calculate the neutrino emission rates for the standard and several nonstandard interaction models, it remains to calculate the decay rates for the process $\gamma_s \to \bar{\nu}\nu$. In the standard model one finds (Adams, Ruderman, & Woo 1963; Zaidi 1965; Dicus 1972)

$$\Gamma_{s,k} = C_V^2\frac{G_F^2}{48\pi^2\alpha}\frac{Z_{s,k}\,\pi_{s,k}^3}{\omega_{s,k}}\,. \tag{10}$$

The effective vector coupling constant is

$$C_V^2 \equiv \sum_{i=1}^{3}C_{V,i}^2 = (\tfrac{1}{2} + 2\sin^2\Theta_W)^2 + 2(\tfrac{1}{2} - 2\sin^2\Theta_W)^2\,, \tag{11}$$

where $C_{V,i}$ is the effective neutral-current vector coupling con-

[2] Our $Z_{L,k}^*$ is what Braaten & Segel (1993) call $Z_L(k)$.

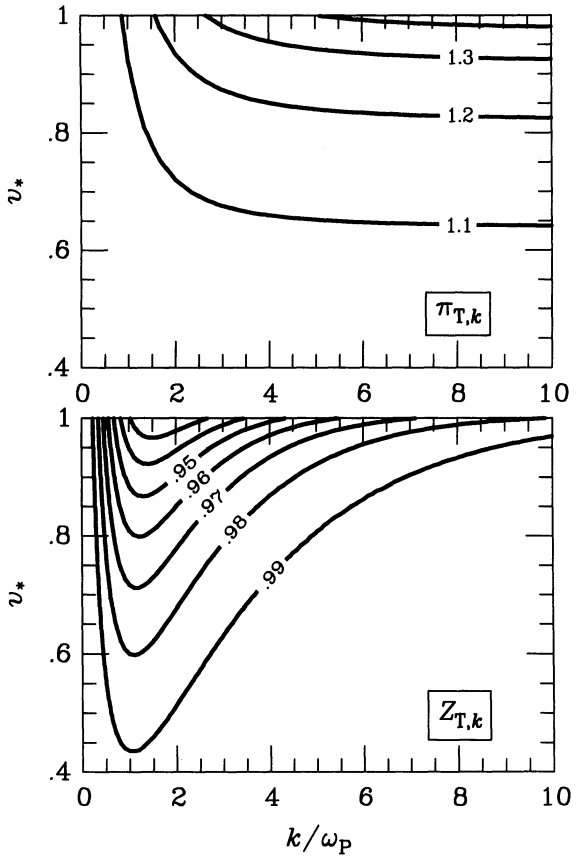

FIG. 4.—Contours for $\pi_{T,k} = \omega_{T,k}^2 - k^2$ in units of ω_P^2 and for $Z_{T,k}$

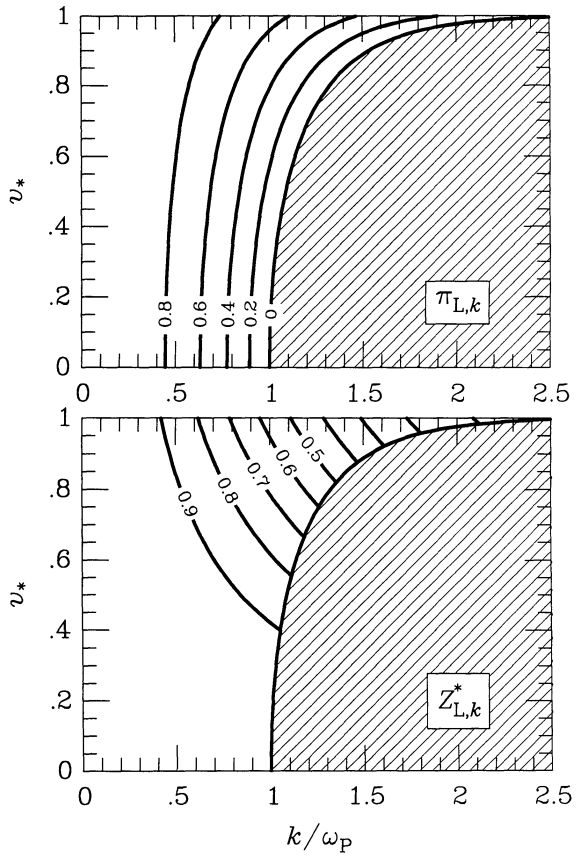

FIG. 5.—Contours for $\pi_{L,k} = \omega_{L,k}^2 - k^2$ in units of ω_P^2 and for $Z^*_{L,k} = Z_{L,k}\pi_{L,k}/\omega_{L,k}^2$. The $\pi_{L,k} = 0$ contour corresponds to $k_{max}(v_*)$ of eq. (9). In the hatched region longitudinal plasmons have a spacelike four-momentum and thus cannot decay.

stant of neutrino flavor i to the electrons. With a weak mixing angle of $\sin^2 \Theta_W = 0.2325 \pm 0.0008$, this is $C_V^2 = (0.9312 \pm 0.0031) + 2(0.0012 \pm 0.0001) = 0.9325 \pm 0.0033$, where the first term is from $\gamma_s \to \bar{\nu}_e \nu_e$, while the second term is from $\bar{\nu}_\mu \nu_\mu$ and $\bar{\nu}_\tau \nu_\tau$. Thus, even if these latter flavors were too heavy to be produced by plasmon decay, the value of C_V^2 would change by less than its uncertainty. The contribution of the axial neutral current is always negligible.

As a first nonstandard coupling, we consider a model by Fukugita & Yanagida (1990) which was devised to obtain a large neutrino magnetic dipole moment and a strong effective coupling of right-handed ν_e's to electrons. The relevant part of the Lagrangian is

$$\mathcal{L}_{\nu_R e_L} = g\phi\bar{\psi}_{\nu_R}\psi_{e_L} + \text{h.c.}\,, \tag{12}$$

where ϕ is a scalar field of mass m, g is a dimensionless coupling constant, and h.c. is the Hermitian conjugate. For low energies this interaction produces an effective neutral-current coupling of right-handed neutrinos to electrons. The corresponding effective vector coupling constant is

$$C_{V,R}^2 = \frac{g^4}{32m^4 G_F^2}\,. \tag{13}$$

In this model the rate for $\gamma_s \to \bar{\nu}_{e,R}\nu_{e,R}$ is found by inserting $C_{V,R}^2$ instead of C_V^2 into equation (10).

Next, we consider direct couplings of neutrinos with the electromagnetic field. The least exotic possibility is that of neutrino dipole moments with an effective Lagrangian

$$\mathcal{L}_\mu = \tfrac{1}{2}\sum_{i,j=1}^{3}(\mu_{ij}\bar{\psi}_i\sigma_{\mu\nu}\psi_j + \epsilon_{ij}\bar{\psi}_i\sigma_{\mu\nu}\gamma_5\psi_j)F^{\mu\nu}\,, \tag{14}$$

where μ_{ij} and ϵ_{ij} are matrices of magnetic and electric dipole and transition moments, F is the electromagnetic field tensor, and the sum is over neutrino flavors. We define an effective dipole moment by

$$\mu_\nu^2 \equiv \sum_{i,j=1}^{3}(|\mu_{ij}|^2 + |\epsilon_{ij}|^2)\,, \tag{15}$$

with the restriction that the sum should only run over those flavors which are light enough to be produced by the plasma process: $m_i + m_j \lesssim \omega_P$. Then we find for the plasmon decay rate

$$\Gamma_{s,k} = \frac{\mu_\nu^2}{24\pi}\frac{Z_{s,k}\pi_{s,k}^2}{\omega_{s,k}}\,. \tag{16}$$

This result is in agreement with Sutherland et al. (1976) except for their $Z_{L,k}$.

Finally, we assume that neutrino flavor i carries a "millicharge" $q_i e$. In this case we find

$$\Gamma_{s,k} = \frac{q_\nu^2\alpha}{3}\frac{Z_{s,k}\pi_{s,k}}{\omega_{s,k}}\,, \tag{17}$$

where $\alpha = e^2/4\pi$ is the (electron) fine-structure constant and $q_v^2 \equiv \sum_{i=1}^{3} q_i^2$.

2.4. *Neutrino Emission Rates*

If transverse and longitudinal electromagnetic excitations of momentum k can decay according to $\gamma_s \to \bar{\nu}\nu$ with a rate $\Gamma_{s,k}$, then the energy loss rate per unit volume of a medium at temperature T is $Q = Q_T + Q_L$, where

$$Q_T = 2\int_0^\infty \frac{dk\,k^2}{2\pi^2}\frac{\Gamma_{T,k}\,\omega_{T,k}}{e^{\omega_{T,k}/T}-1}\,,$$
$$Q_L = \int_0^{k_{\max}} \frac{dk\,k^2}{2\pi^2}\frac{\Gamma_{L,k}\,\omega_{L,k}}{e^{\omega_{L,k}/T}-1}\,. \tag{18}$$

Inserting the results of the previous section in this equation, we find for the various interaction models

$$Q_V = C_V^2\,\frac{G_F^2}{96\pi^4\alpha}\,T^3\omega_P^6\,Q_3\,,$$
$$Q_\mu = \frac{\mu_\nu^2}{48\pi^3}\,T^3\omega_P^4\,Q_2\,, \tag{19}$$
$$Q_q = \frac{q_v^2\,\alpha}{6\pi^2}\,T^3\omega_P^2\,Q_1\,.$$

The dimensionless emission rates are $Q_n \equiv (Q_n^T + Q_n^L)$, where

$$Q_n^T \equiv 2\int_0^\infty \frac{dk\,k^2}{T^3}\,Z_{T,k}\left(\frac{\pi_{T,k}}{\omega_P^2}\right)^n \frac{1}{e^{\omega_{T,k}/T}-1}\,,$$
$$Q_n^L \equiv \int_0^{k_{\max}} \frac{dk\,k^2}{T^3}\,Z_{L,k}\left(\frac{\pi_{L,k}}{\omega_P^2}\right)^n \frac{1}{e^{\omega_{L,k}/T}-1}\,. \tag{20}$$

In the Braaten & Segel approximation the Q_n^s are only functions of v_* and $\gamma = \omega_P/T$.

In Figure 6 we show contours in the (v_*, γ)-plane of Q_3^L/Q_3^T, i.e., the ratio between longitudinal and transverse emissivity for the standard model interactions. Corresponding contours in the (ρ, T)-plane are shown as dashed lines in Figure 1. Evidently, the longitudinal process is of importance only in a relatively narrow region near $\gamma = 10$.

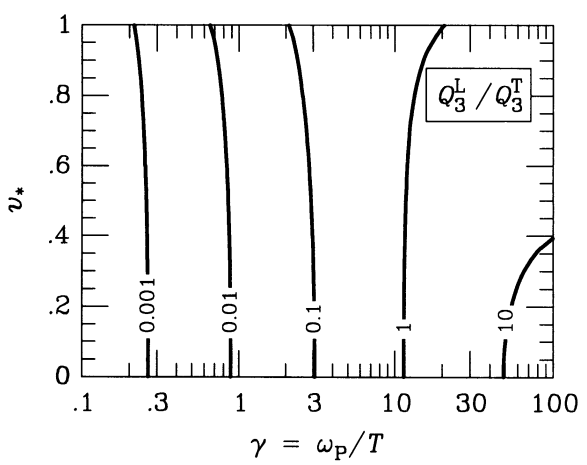

FIG. 6.—Contours for Q_3^L/Q_3^T as defined in eq. (20). This ratio is identical to the ratio of the longitudinal and transverse emission rates in the standard model.

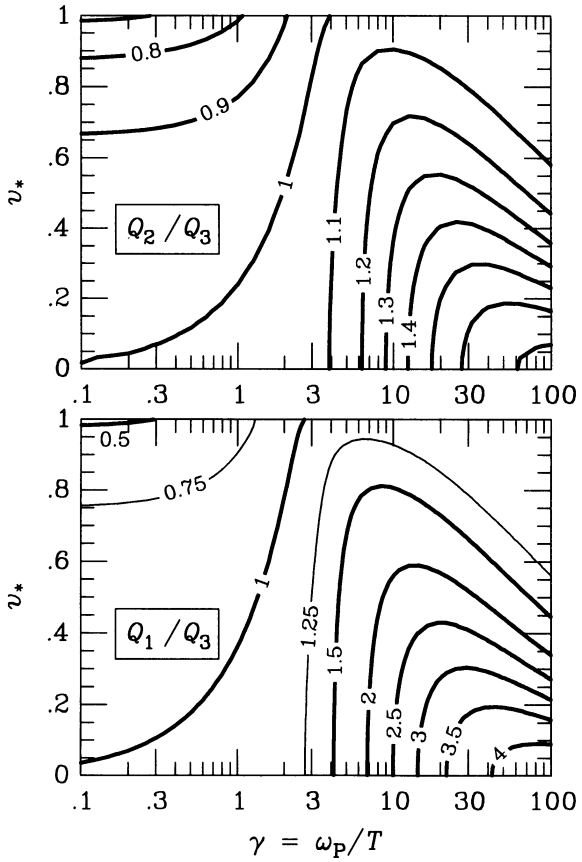

FIG. 7.—Contours for Q_2/Q_3 and Q_1/Q_3 as defined in eq. (20)

In a practical calculation of anomalous neutrino losses, one will scale the standard luminosity appropriately. The relevant ratios are

$$\frac{Q_\mu}{Q_V} = \frac{\mu_\nu^2\,2\pi\alpha}{C_V^2\,G_F^2\,\omega_P^2}\,\frac{Q_2}{Q_3} = 0.318\mu_{12}^2\left(\frac{10\text{ keV}}{\omega_P}\right)^2\frac{Q_2}{Q_3}\,, \tag{21}$$

where $\mu_{12} \equiv \mu_\nu/10^{-12}(e/2m_e)$, and

$$\frac{Q_q}{Q_V} = \frac{q_v^2(4\pi\alpha)^2}{C_V^2\,G_F^2\,\omega_P^4}\,\frac{Q_1}{Q_3} = 0.664q_{14}^2\left(\frac{10\text{ keV}}{\omega_P}\right)^4\frac{Q_1}{Q_3}\,, \tag{22}$$

where $q_{14} \equiv q_\nu/10^{-14}$. In Figure 7 we show contours of Q_1/Q_3 and Q_2/Q_3.

3. NUMERICAL EMISSION RATES

Even though the methods described in § 2 allow for a relatively simple calculation of the plasma neutrino emission rates, one still needs to evaluate several numerical integrals in order to determine the energy loss rate for given values of density and temperature, so that this procedure is not suitable to be coupled directly with a stellar evolution code. However, we can use these results to test the accuracy of widely used analytic approximation formulae.

It turns out that for the plasma process the analytic approximations of Beaudet et al. (1967), Munakata et al. (1985), and Schinder et al. (1987) all agree with each other to an astonishing accuracy if the same value for C_V^2 is used. In Figure 8*a* we compare the numerical rates of Beaudet et al. (1967) with the exact results obtained by the Braaten & Segel method. We

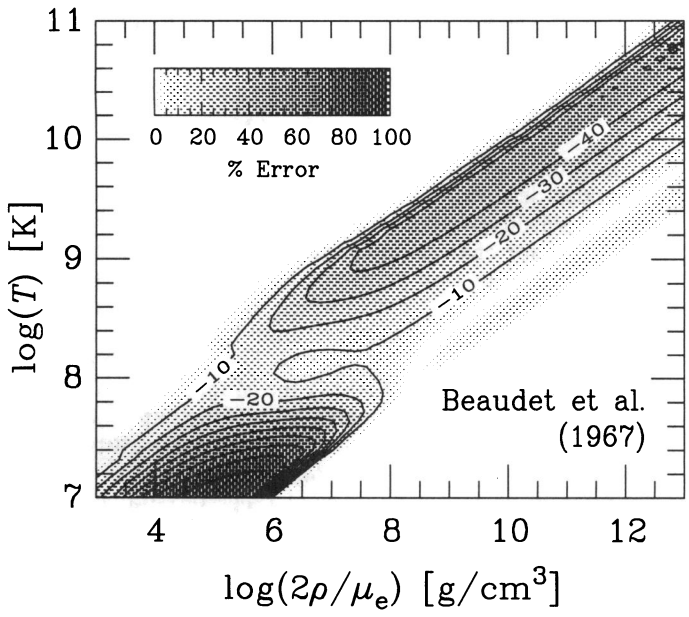

FIG. 8a

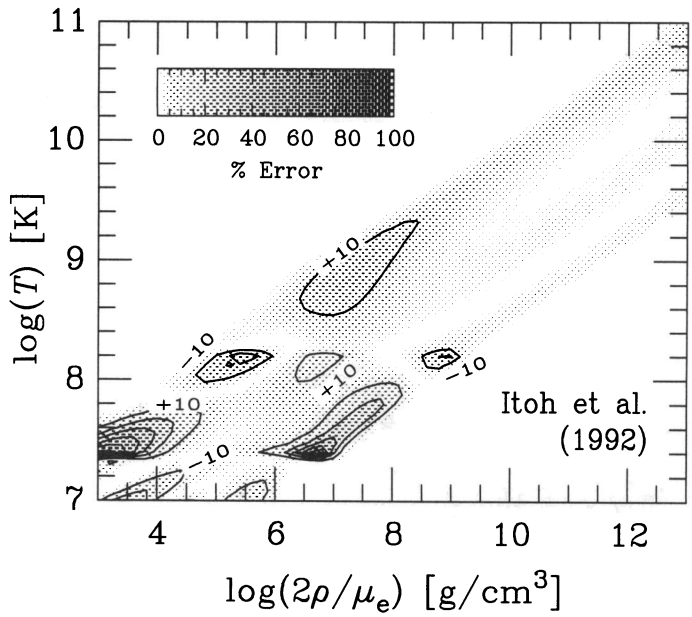

FIG. 8b

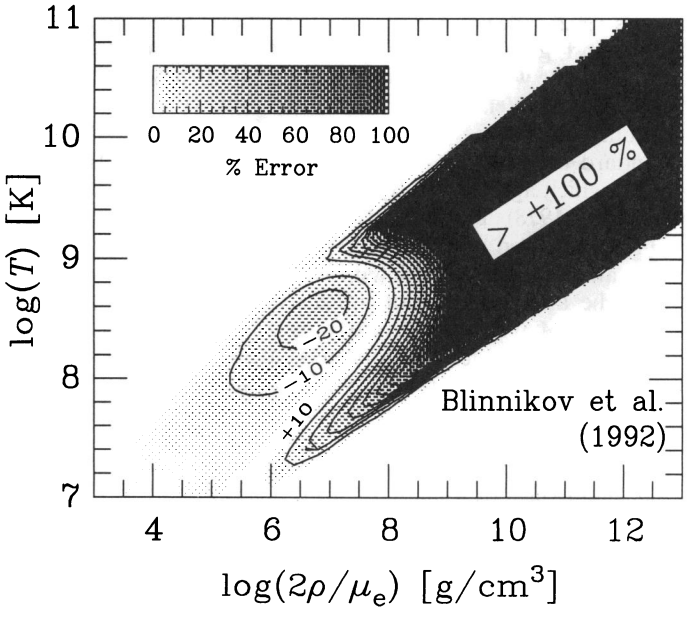

FIG. 8c

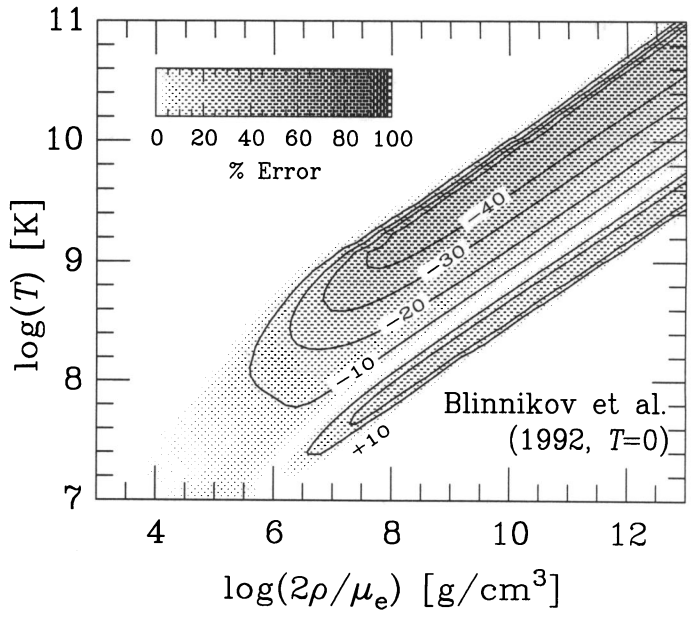

FIG. 8d

FIG. 8.—(*a*)–(*e*) Comparison of the analytic plasma emission rates of the indicated authors with the exact rates. Except for (*e*), the contours are at multiples of ±10%. The errors in (*a*) of the Beaudet et al. (1967) rates are the same for Munakata et al. (1985) and Schinder et al. (1987).

show contours for the relative deviation in percent, $Q^{\rm tot}_{\rm analytic}/Q^{\rm tot}_{\rm exact} - 1$. We stress that what is plotted is the error of the *total* emission rate; the plasma process alone may be more inaccurate than shown in regions where it does not dominate. In this and the following figures we have used the rates of Itoh et al. (1989) for the other emission processes. Thus, $Q^{\rm tot}_{\rm analytic}$ and $Q^{\rm tot}_{\rm exact}$ differ only in the treatment of the plasma process. From Figure 8*a* it is evident that the numerical rates are rather poor approximations almost everywhere. Nevertheless, it is these rates that have been used in virtually all stellar evolution calculations.

Recently Itoh et al. (1992) have published numerical rates for the plasma process which are claimed to be more accurate than 5% wherever the plasma process dominates. In Figure 8*b* we put this claim to a test and find that there remain substantial regions with much larger errors. We have checked that at least some of these deviations also occur between their tabulated emission rates and their fitting formula.

Blinnikov & Dunina-Barkovskaya (1992) have also derived a new analytic approximation which is optimized in the region of small temperatures and densities relevant for low-mass stars. We compare their rates with the exact ones in Figure 8*c*. Indeed, these rates are rather good fits for $T \lesssim 10^8$ K and $\rho \lesssim 10^6$ g cm^{-3}, but for higher T or ρ they are unrelated to the exact results. These approximation formulae involve multiplicative factors which depend on T alone and which approach

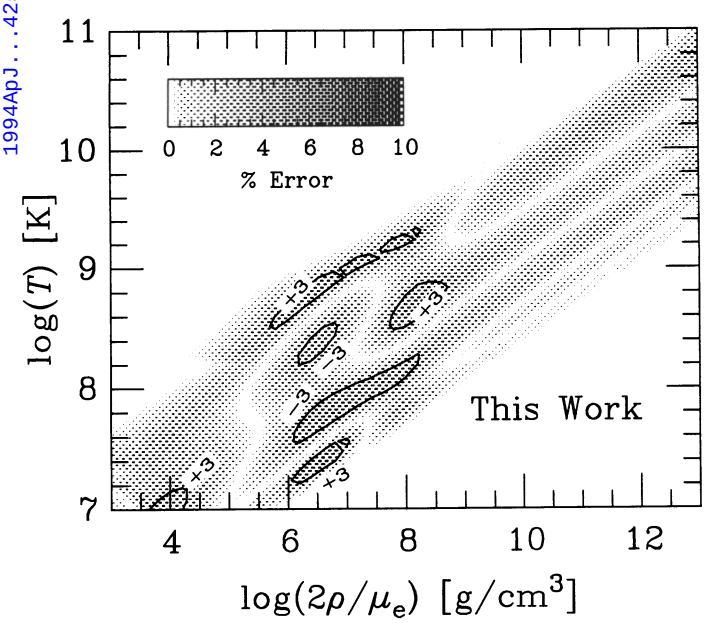

FIG. 8e

unity for $T \to 0$. If we set these factors to unity for all T, the errors of the resulting simplified emission rates are shown in Figure 8*d*. The fit is not worse in the low-T and low-ρ region, and much better otherwise!

Since we find none of the published fitting formulae satisfactory, we have derived a new one. To this end we have started with the $T = 0$ version of Blinnikov & Dunina-Barkovskaya (1992) and then "flattened" the errors with an extra correction factor f_{xy}. As a result we have come up with $Q_{\rm plas} = C_V^2 Q_{\rm approx}$ (in ergs cm^{-3} s^{-1}), where

$$Q_{\rm approx} = 3.00 \times 10^{21} \lambda^9 \gamma^6 e^{-\gamma} (f_T + f_L) f_{xy} , \qquad (23)$$

where $\lambda = T/m_e$ and $\gamma = \omega_0/T$, where ω_0 is the zero-temperature plasma frequency, $\omega_0^2 = 4\pi\alpha N_e/E_{\rm F}$. Numerically,

$$\lambda = 1.686 \times 10^{-10} T ,$$
$$\gamma^2 = \frac{1.1095 \times 10^{11} \rho/\mu_e}{T^2 [1 + (1.019 \times 10^{-6} \rho/\mu_e)^{2/3}]^{1/2}} , \qquad (24)$$

with T in K, ρ in g cm^{-3}, and μ_e the number of baryons per electron. Moreover, we have

$$f_T = 2.4 + 0.6\gamma^{1/2} + 0.51\gamma + 1.25\gamma^{3/2} ,$$
$$f_L = \frac{8.6\gamma^2 + 1.35\gamma^{7/2}}{225 - 17\gamma + \gamma^2} . \qquad (25)$$

The coefficients here are slightly different from those used by Blinnikov & Dunina-Barkovskaya (1992). Finally, we define

$$x = \tfrac{1}{6}[+17.5 + \log_{10}(2\rho/\mu_e) - 3 \log_{10}(T)] ,$$
$$y = \tfrac{1}{6}[-24.5 + \log_{10}(2\rho/\mu_e) + 3 \log_{10}(T)] , \qquad (26)$$

where x is a coordinate transverse to the diagonal band in Figure 1 where the plasma process is important, and y is along this band. If $|x| > 0.7$ or $y < 0$, we use $f_{xy} = 1$, and otherwise

$$f_{xy} = 1.05 + \{0.39 - 1.25x - 0.35 \sin(4.5x) - 0.3 \exp[-(4.5x + 0.9)^2]\} \times \exp\left\{-\left[\frac{\min(0, y - 1.6 + 1.25x)}{0.57 - 0.25x}\right]^2\right\} . \qquad (27)$$

We show the errors of our fitting formula in Figure 8*e*; it is better than 5% everywhere and better than 4% almost everywhere.

4. DISCUSSION AND SUMMARY

In low-mass stars helium ignites in the cores of red giant stars under degenerate conditions. Helium burning depends extremely sensitively on temperature and density, so that even relatively minor changes in the neutrino cooling rates of the core change the ignition point and thus the core mass $M_{\rm tip}$ at the tip of the red giant branch, which in turn affects the luminosity during the subsequent horizontal-branch evolution. All previous calculations of the core mass at helium flash seem to have used the Beaudet et al. (1967), the Munakata et al. (1985), or the Schinder et al. (1987) rates, all of which are equivalent with regard to the plasma process and thus underestimate the emission rate as shown in Figure 8*a*.

In order to illustrate the relevant range of parameters, we show in Figure 9 the evolution of the central density and temperature of a 0.80 $M_\odot$ star, where the tail ends of the arrows mark the conditions when the surface brightness is at the indicated magnitudes. In Figure 10 we show the red giant part of this track overlaid with the errors of the Munakata et al. (1985) rates that were used in our previous calculations (Raffelt & Weiss 1992). The error contours are virtually the same as those shown in Figure 8*a*. Near the helium flash the average neutrino emission rate was underestimated by around 15%.

Raffelt & Weiss (1992) found that the core mass at the helium flash varies approximately as $\delta M_c = 0.020 \delta F_\nu$ if the standard neutrino loss rates are multiplied by a factor F_ν, a result which agrees with the previous calculations of Sweigart & Gross (1978). Therefore, the core mass at the helium flash will be increased by about 0.004 $M_\odot$. In order to confirm this estimate, we have recalculated run 11 of Raffelt & Weiss (1992) with the analytic emission rates derived in this paper. For $M = 0.80\ M_\odot$, $Z = 10^{-4}$, and $Y_0 = 0.22$, we previously found $M_{\rm tip} = 0.497\ M_\odot$ for the core mass at helium ignition (at the tip of the red giant branch), while we now find $M_{\rm tip} = 0.503\ M_\odot$. Therefore, we find an increase of $\delta M_{\rm tip} = 0.006\ M_\odot$, in reasonable agreement with our simple estimate. Thus, using the correct neutrino emission rates changes the core mass at the helium flash by a small but noticeable amount.

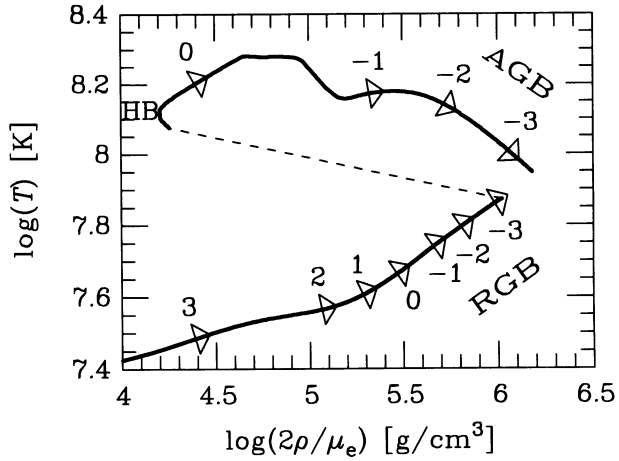

FIG. 9.—Evolution of the central density and temperature of a 0.80 $M_\odot$ star up the red giant branch (RGB), and then from the horizontal branch (HB) up the asymptotic giant branch (AGB). The rear ends of the arrows are at the indicated values for the surface brightness.

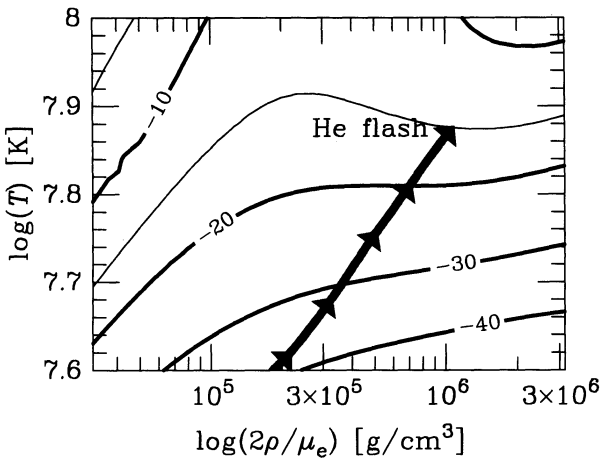

FIG. 10.—Error in percent of the standard neutrino emission rates used in the evolutionary calculations of Raffelt & Weiss (1992). The evolutionary track is that of Fig. 9.

In order to constrain neutrino dipole moments, Raffelt & Weiss (1992) as well as Blinnikov & Dunina-Barkovskaya (1992) and Castellani & Degl'Innocenti (1992) have included the increased plasma losses in evolutionary calculations by scaling the standard rates with a certain factor. Instead of the exact ratio given by equation (21), they used $Q_2/Q_3 = 1$ and $\omega_P^2 = \omega_0^2 = 4\pi\alpha N_e/E_F$, which is the zero-temperature value for the plasma frequency. In Figure 11 we show the evolutionary track of Figure 9 in the plane of $\gamma = \omega_P/T$ and v_*. Evidently on the red giant branch the interior of the core has an almost constant value $\gamma \approx 3$. A comparison with the upper panel of Figure 7 reveals that by using $Q_2/Q_3 = 1$ Raffelt & Weiss (1992) have underestimated the dipole-induced emission rate by about 5%. An additional small error occurs by using ω_0 instead of ω_P. In Figure 12 (*upper panel*) we show the error of the dipole-induced emission rate if it had been scaled with the correct standard rate. These errors are so small that this scaling procedure remains well justified.

In Figure 12 (*lower panel*) we show the compound error of the dipole-induced emission rate when coupled with the Munakata et al. (1985) emission rates. Near helium ignition the emission rate was underestimated by 15%–20%. Because the

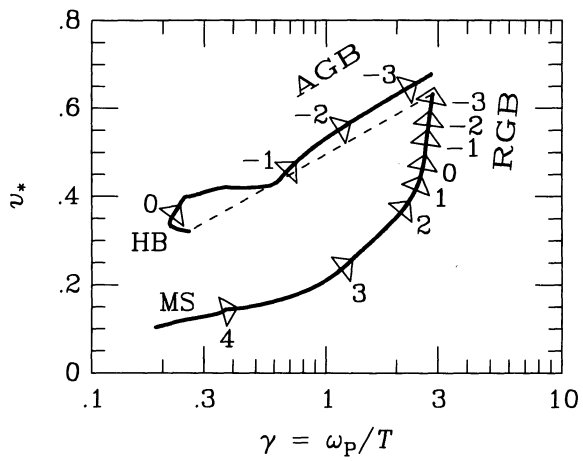

FIG. 11.—Evolutionary track of Fig. 9 in the (γ, v_*)-plane

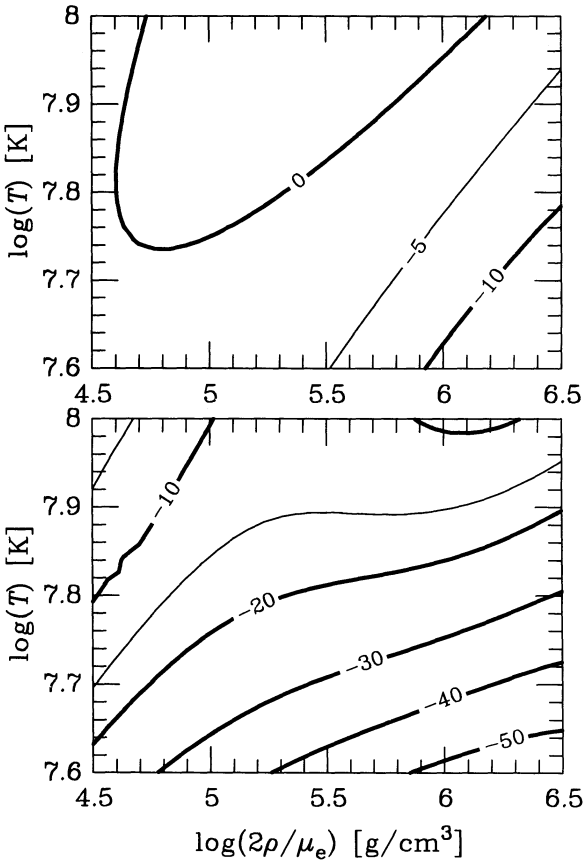

FIG. 12.—Error in percent of the dipole moment emission rates used in the calculations of Raffelt & Weiss (1992). *Upper panel:* Error relative to the standard rates. *Lower panel:* Compound error if combined with the analytic standard rates of Munakata et al. (1985).

core mass and brightness at the helium flash vary approximately linearly with μ_ν in the range of interest, for a given value of μ_ν these quantities are changed by about 10% more than given in Raffelt & Weiss (1992). This is a negligible change with regard to bounds on μ_ν.

The bounds on neutrino dipole moments discussed in Raffelt (1990) and Raffelt & Weiss (1992) crudely amount to the constraint that the total neutrino luminosity must not exceed about twice its standard value in order to maintain the beautiful agreement between the observed and calculated properties of globular cluster stars. We have already discussed that on the red giant branch we may set $Q_2/Q_3 = 1$ in equation (21) without introducing a large error, and similarly we may set $Q_1/Q_3 = 1$ in equation (22), although the error here is somewhat larger. In any case, these approximations lead to an underestimation of the nonstandard emission rates and thus to conservative bounds. Moreover, near the helium flash the density is about 10^6 g cm^{-3} (see Fig. 10), so that $\omega_P^2 = 17.8$ keV in the center of the star. Therefore, in the center of the star we have for the total energy loss rate from equations (21) and (22)

$$Q_{\rm tot}/Q_V = 1 + 1.07C_{V,R}^2 + 0.100\mu_{12}^2 + 0.066q_{14}^2 . \quad (28)$$

Away from the center the density and thus ω_P are lower, so that the coefficients of μ_{12}^2 and of q_{14}^2 would be larger if averaged properly over the core. Hence this expression, again, is a conservative estimate of the nonstandard neutrino losses. With

$Q_{\rm tot}/Q_V < 2$ as a formal criterion, we find the bounds

$$C_{V,R} < 0.9\,,$$
$$\mu_\nu < 3 \times 10^{-12}(e/2m_e)\,, \qquad (29)$$
$$q_\nu < 4 \times 10^{-14}\,.$$

In the model of Fukugita & Yanagida (1990), one has both a dipole moment and right-handed interactions for the ν_e's, so that in that model the constraints on the dipole moment are more restrictive. The bound on μ_ν alone is virtually the same as that from the more detailed analysis of Raffelt (1990) and Raffelt & Weiss (1992). The bound on q_ν is slightly more restrictive than that found by Bernstein, Ruderman, & Feinberg (1963).

In summary, we have discussed in detail the neutrino emission rates from the plasma process due to standard and nonstandard interactions. By means of Braaten & Segel's (1993) representation of the QED dispersion relations we have tested the accuracy of widely used analytic approximation formulae, none of which are found satisfactory. For the first time we have derived an approximation formula which is accurate on the 4% level wherever the plasma process dominates. The correct emission rate leads to a slightly increased core mass at the helium flash in low-mass stars, and to a slightly increased sensitivity to nonstandard neutrino losses. While these changes are noticeable, they are so small that previous bounds on neutrino dipole moments remain virtually unchanged.

REFERENCES

Adams, J. B., Ruderman M. A., & Woo, C.-H. 1963, Phys. Rev., 129, 1383
Beaudet, G., Petrosian, V., & Salpeter, E. E. 1967, ApJ, 150, 979
Bernstein, J., Ruderman, M., & Feinberg, G. 1963, Phys. Rev., 132, 1227
Blinnikov, S. I., & Dunina-Barkovskaya, N. V. 1994, MNRAS, 266, 289
Braaten, E. 1991, Phys. Rev. Lett., 66, 1655
Braaten, E., & Segel, D. 1993, Phys. Rev. D, 48, 1478
Castellani, V., & Degl'Innocenti, S. 1992, ApJ, 402, 574
Dicus, D. A. 1972, Phys. Rev. D, 6, 961
Fukugita, M., & Yanagida, T. 1990, Phys. Rev. Lett., 65, 1975
Itoh, N., Adachi, T., Nakagawa, M., Kohyama, Y., & Munakata, H. 1989, ApJ, 339, 354; 360, 741 (1990)
Itoh, N., Mutoh, H., Hikita, A., & Kohyama, Y. 1992, ApJ, 395, 622
Munakata, H., Kohyama, Y., & Itoh, N. 1985, ApJ, 296, 197; 304, 580 (1986)
Nieves, J., & Pal, P. B. 1989a, Phys. Rev. D, 39, 652
———. 1989b, Phys. Rev. D, 40, 1350
Raffelt, G. 1990, ApJ, 365, 559
Raffelt, G., & Weiss, A. 1992, A&A, 264, 536
Schinder, P. J., Schramm, D. N., Wiita, P. J., Margolis, S. H., & Tubbs, D. L. 1987, ApJ, 313, 531
Sutherland, P., et al. 1976, Phys. Rev. D, 13, 2700
Sweigart, A. V., & Gross, P. G. 1978, ApJS, 36, 405
Weldon, H. A. 1982, Phys. Rev. D, 26, 1394
Zaidi, M. H. 1965, Nuovo Cimento, 40A, 502